Coupling of interfacial and spin-like coordinates in effective Hamiltonians for complete and critical wetting

2001 J. Phys. A: Math. Gen. 34 961

(http://iopscience.iop.org/0305-4470/34/5/303)

INSTITUTE OF PHYSICS PUBLISHING JOURNAL OF PHYSICS A: MATHEMATICAL AND GENERAL

J. Phys. A: Math. Gen. **34** (2001) 961–979 www.iop.org/Journals/ja PII: S0305-4470(01)16961-1

Coupling of interfacial and spin-like coordinates in effective Hamiltonians for complete and critical wetting

C J Boulter

Department of Mathematics, Heriot-Watt University, Edinburgh EH14 4AS, UK

Received 9 September 2000, in final form 4 December 2000

Abstract

In this paper the effects of including position-dependent stiffness coefficients in the coupled effective Hamiltonian models appropriate for both complete and critical wetting are considered. This analysis is motivated by a nonlinear functional renormalization group approach applied for the first time to two-field interface models, and cast in a simple matrix form. In particular we (i) determine the renormalization group flow of the capillary parameter and confirm that its renormalization at complete wetting is preserved at all orders and (ii) demonstrate that the stiffness instability mechanism is robust, and indeed strengthened, under the inclusion of coupling terms near critical wetting.

PACS numbers: 6845G, 6460A, 8265D

1. Introduction

In recent years there have been a number of developments in the field of wetting transitions for systems with short-ranged forces [1][1]. These advances have primarily been driven by inconsistencies between Monte Carlo simulation studies and theoretical renormalization group (RG) predictions for critical wetting in three dimensions, and by the failure of simple interface models to correctly describe known correlation function behaviour [2, 3][2].

Although progress has been made in understanding these various problems individually by introducing appropriately modified interface Hamiltonian models, a unified analysis which incorporates all of the changes has been lacking. In particular, a detailed study of the effect of coupling terms on fluctuation behaviour has not been possible due to the absence of a suitable nonlinear RG scheme which could be applied to interface models including position-dependent stiffness coefficients. In this paper we introduce such a scheme suitable for the coupled 'two-field' models that are a necessary ingredient of a complete theory. Using this tool we are able to show that the renormalization of the wetting parameter, which has been a crucial feature in understanding Monte Carlo simulation results, remains robust under the

[1] For a general review of wetting, see, for example, [1].

[2] For a comprehensive discussion, see [2].

0305-4470/01/050961+19$30.00

inclusion of position-dependent stiffnesses. Furthermore, close to critical wetting we show that the various components of the stiffness matrix couple in a complex fashion not accessible in linear studies. To quantify the importance of this coupling we derive an 'effective one-field' interface model and find that the Fisher–Jin stiffness instability mechanism is strengthened, an effect directly attributable to the original coupling terms.

The remainder of the paper is organized as follows. In the next section we briefly recall some pertinent recent advances in effective interface Hamiltonian theories for wetting transitions. In section 3 a nonlinear RG scheme for an arbitrary coupled model is introduced, the key results of which can be conveniently written in terms of the stiffness matrix. In section 4 this scheme is then applied to study the effect of position-dependent stiffnesses and coupling on complete and critical wetting. Finally a discussion and summary of the main results is given in section 5.

2. Effective interface Hamiltonians

In this section we highlight the relevant recent advances in the theory of effective interface Hamiltonian models applied to wetting transitions. At such a transition the thickness, l, of an adsorbed layer diverges as some parameter is varied towards its critical value. For concreteness consider a semi-infinite system with a wall in the plane $z = 0$. Using magnetic notation we assume that in zero bulk field ($h = 0$) there are two coexisting bulk phases ($\alpha \equiv$ 'downspins', $\beta \equiv$ 'upspins') while the wall preferentially favours the β-phase. If wetting occurs in a given system one can identify a corresponding sub-critical wetting temperature T_W. The divergence of the thickness l may occur discontinuously at T_W indicating a first-order wetting transition, or l may diverge continuously as $T \to T_W$ indicating a continuous or second-order transition. In this latter case we can consider two different routes to approach wetting: (i) *critical wetting* corresponding to letting the temperature T approach T_W from below while maintaining bulk coexistence $h = 0-$, and (ii) *complete wetting* corresponding to letting the bulk field approach zero from the negative side at some fixed temperature $T > T_W$. For systems with short-ranged forces the upper critical dimension for both transitions is $d = 3$ so that the effect of fluctuations is important for this most physically interesting case. In order to enable RG studies of these fluctuation effects it has proved convenient to introduce simple effective interface models, which are functionals of the layer thickness. The traditional starting point is the capillary wave model [4–6]

$$\mathcal{H}_{\mathrm{CW}}[l] = \int \mathrm{d}\boldsymbol{y}\, \{\tfrac{1}{2}\Sigma_{\alpha\beta}(\nabla l)^2 + W(l)\} \tag{1}$$

where $W(l) \equiv W(l; T, h, \ldots)$ is the binding potential or effective wall–interface interaction, which takes the form $W(l) = \bar{h}l + a(T, h, \ldots)\mathrm{e}^{-\kappa l} + b\mathrm{e}^{-2\kappa l} + \cdots$. Here $\bar{h} \sim -h$, $\kappa \equiv 1/\xi_b$ is the inverse bulk correlation length of the wetting phase, the parameter $a \sim (T - T_W^{\mathrm{MF}})$ in zero bulk field (where T_W^{MF} is the mean-field (MF) critical wetting temperature) and b is strictly positive in the vicinity of a continuous transition. At the MF level the location of the interface is simply given by the minimum of $W(l)$. The coefficient of the gradient term in (1) is the interfacial stiffness, which is approximated by $\Sigma_{\alpha\beta}$, the stiffness of a free $\alpha\beta$ interface.

2.1. The Fisher–Jin stiffness instability mechanism

More recently Fisher and Jin (FJ) have questioned the phenomenological expression (1) and in particular the presence of an l-independent stiffness coefficient [7, 8]. Instead they aimed at

deriving an interface model from an underlying bulk theory, typically the Landau–Ginzburg–Wilson (LGW) model

$$\mathcal{H}_{\mathrm{LGW}}[m] = \int_{z\geqslant 0} \mathrm{d}\boldsymbol{r}\, \{\tfrac{1}{2}K(\nabla m)^2 + \Phi(m) + \delta(z)\phi_1(m)\} \tag{2}$$

where $m(\boldsymbol{r})$ is the bulk order parameter and $\Phi(m)$ is the bulk free-energy density, which has a double-well form. The surface potential ϕ_1 is typically represented by a truncated expansion of the form $\phi_1(m) \approx -h_1 m + cm^2/2$, where h_1 and c are the surface field and enhancement respectively. A constraint is introduced which restricts order-parameter profiles to those consistent with a given interface configuration $l(\boldsymbol{y})$. The interface Hamiltonian is then defined in a saddle-point treatment via $\mathcal{H}_{\mathrm{FJ}}[l] = \min^{l}_{m(\boldsymbol{r})} \mathcal{H}_{\mathrm{LGW}}[m]$, where $\min^{l}_{m(\boldsymbol{r})}$ identifies the profile $m(\boldsymbol{r})$ which minimizes $\mathcal{H}_{\mathrm{LGW}}$ subject to the interface constraint. The simplest criterion to define the interface is a crossing constraint which demands that $m(z = l(\boldsymbol{y}), \boldsymbol{y}) = m^X$, where typically the crossing magnetization m^X is set to zero. Using this approach FJ find

$$\mathcal{H}_{\mathrm{FJ}}[l] = \int \mathrm{d}\boldsymbol{y}\, \{\tfrac{1}{2}\Sigma(l)(\nabla l)^2 + W(l)\} \tag{3}$$

where the stiffness coefficient $\Sigma(l)$ now displays a position dependence. In terms of planar constrained profiles $m_\pi(z; l)$, this contribution may be written as

$$\Sigma(l) = \Sigma_{\alpha\beta} + \Delta\Sigma(l) = \int_0^\infty \mathrm{d}z \left(\frac{\partial m_\pi(z; l)}{\partial l}\right)^2 \tag{4}$$

where we have explicitly identified the position-dependent contribution, $\Delta\Sigma(l)$, which must vanish in the limit $l \to \infty$. Similarly, the binding potential $W(l)$ is given (up to l-independent terms) by

$$W(l) = \int_0^\infty \mathrm{d}z \left\{\frac{1}{2}K\left(\frac{\partial m_\pi(z; l)}{\partial z}\right)^2 + \Delta\Phi(m_\pi)\right\} + \Phi_1(m_\pi(z = 0; l)). \tag{5}$$

Here $\Delta\Phi(m)$ Φ_{min} denotes the minimum value of $\Phi(m)$.

The crucial difference between (3) and the capillary wave model (1) is the position-dependent stiffness contribution[3] $\Delta\Sigma(l)$, which at leading orders can be expanded $\Delta\Sigma(l) = s(T, h, \ldots)\mathrm{e}^{-\kappa l} - q(\kappa l)\mathrm{e}^{-2\kappa l} + \cdots$ where $s \sim (T - T_W^{\mathrm{MF}})$ and $q > 0$. The importance of this term is seen through RG analyses, which reveal at linear order that the flows of W and $\Delta\Sigma$ are coupled. In particular, for sufficiently large values of the renormalization parameter t, one can consider just an effective binding potential of the form

$$W^{(t)}_{\mathrm{eff}}(l) \approx W^{(t)}(l) + \frac{\omega\Lambda^2}{2\kappa^2}\Delta\Sigma^{(t)}(l) \tag{6}$$

in $d = 3$. Here Λ is a non-universal momentum cutoff implicitly contained within the interface model, while the capillary parameter ω is defined as

$$\omega = \frac{k_{\mathrm{B}}T\kappa^2}{4\pi\,\Sigma_{\alpha\beta}} \tag{7}$$

and is estimated at $\omega \approx 0.8$ near the transition. Thus, if the relative magnitude and sign of terms in W and $\Delta\Sigma$ remain under renormalization, we observe that the next-to-leading-order term in the expansion for $W_{\mathrm{eff}}(l)$ arises through the $\Delta\Sigma(l)$ contribution and is negative, which provides a potential instability mechanism for wetting. In this way a bare critical wetting

[3] We note that the binding potential $W(l)$ derived via the FJ route also contains extra terms not present in the traditional expansion as given after equation (1). However, they are not found to qualitatively affect critical behaviour at the MF level or beyond.

transition may be fluctuation-induced first order and a recent numerical nonlinear RG analysis provides evidence suggesting that this is indeed the case in $d = 3$ for the currently accepted values of ω [9].

This observation is important in light of earlier RG calculations based upon the capillary wave model. Those studies predicted dramatic non-universal behaviour depending strongly on the value of the capillary parameter [4–6]. These predictions have been supported by Monte Carlo simulations of a lattice version of the capillary wave model [10], and by an approximate nonlinear RG analysis of (1) [11]. However, as yet no evidence of such behaviour has been found in Monte Carlo simulations of the underlying model [12], raising doubts over the applicability of the effective interface approach. The FJ stiffness instability mechanism provides an alternative prediction, which may help explain the earlier inconsistencies—future simulation studies focusing on response functions close to the unbinding interface should further clarify the status of the various RG predictions [13].

2.2. Multi-field interface models and correlation functions

Another concern with the capillary wave model has been raised due to its inability to recover known expressions for MF correlation functions. If one is to put faith in the predictions of an interface model used in fluctuation studies it is clearly desirable that the model should give results at MF level consistent with those found from the underlying bulk model. One of the most frequently studied properties of these models is the connected correlation function $G(\boldsymbol{r}_1, \boldsymbol{r}_2) \equiv \langle m(\boldsymbol{r}_1)m(\boldsymbol{r}_2)\rangle - \langle m(\boldsymbol{r}_1)\rangle\langle m(\boldsymbol{r}_2)\rangle$ and in particular its transverse Fourier transform

$$G(z_1, z_2; Q) = \int \mathrm{d}\boldsymbol{y}_{12}\, \mathrm{e}^{\mathrm{i}Q\cdot y_{12}} G(\boldsymbol{r}_1, \boldsymbol{r}_2) \tag{8}$$

where $\boldsymbol{y}_{12}$ is the parallel displacement of the points $\boldsymbol{r}_1$ and $\boldsymbol{r}_2$, and z_i is the perpendicular displacement of point $\boldsymbol{r}_i$ from the wall. Here we focus on the complete wetting transition in the LGW model, although similar comments apply to critical wetting [3]. If one considers the case when z_1 and z_2 are both near the $\alpha\beta$ interface then the MF correlation function has a simple Lorentzian form $G(z_1, z_2; Q) \approx G(z_1, z_2; 0)/(1 + \xi_\parallel^2 Q^2)$, where $\xi_\parallel$ is the transverse correlation length of the interface. In contrast MF studies of correlation functions for particle positions near the wall ($z_1, z_2 \approx 0$) have revealed unexpectedly rich behaviour [14], with, for example,

$$G(0, 0; Q) \approx \frac{k_\mathrm{B}T m_1'^{\,2}}{m_1'(cm_1' - m_1'') + Q^2\left[\Sigma_{w\beta} - \phi_1(m_1) + \frac{\Sigma_{\alpha\beta}+f_\mathrm{sing}}{1+\xi_\parallel^2 Q^2}\right]} \tag{9}$$

where $m_1 \equiv m(z = 0)$ and here primes denote differentiation with respect to z. Here $\Sigma_{w\beta} - \phi_1(m_1)$ represents the stiffness of the wall–β-phase interface, and f_sing is a singular contribution to the total wall–α-phase stiffness, $\Sigma_{w\alpha}$, such that $\Sigma_{w\alpha} = \Sigma_{w\beta} + \Sigma_{\alpha\beta} + f_\mathrm{sing}$. The structure factor (9) is interesting in that it displays a crossover from coherent to intrinsic behaviour; a full discussion can be found in [14]. This behaviour has also recently been observed in the results of extensive lattice gas model calculations [15][4]. Here our aim is simply to motivate the introduction of a multi-field interface Hamiltonian. To this end we note that both the capillary wave model and the FJ model with $m^X = 0$ are unable to recover the non-Lorentzian structure factor at the wall (although both models are suitable for the study of correlations near the unbinding interface).

[4] These authors focus primarily on short-wavelength behaviour; however, reanalysing their data for the long-wavelength case ($Q \to 0$) reveals behaviour fully consistent with (9).

Parry showed that for the FJ model this problem may be overcome if one makes use of the freedom of choice of reference value m^X [16]. In particular he showed that if $\tilde{m}(z)$ is the (planar) MF profile found from minimizing (2) without constraint, then the FJ model derived with the choice $m^X = \tilde{m}(z_1)$ will exactly rederive the MF structure factor $G(z_1, z_1; Q)$. The failure of the usual models to derive the surface structure factor may be understood by noting that in the complete-wetting limit there are two distinct behaviours for surfaces of fixed magnetization m^X. If m^X lies between the bulk magnetizations of the two phases (i.e. $m_\beta > m^X > m_\alpha$) then the corresponding interface diverges in the limit of complete wetting and will provide a qualitatively sensible representation of the unbinding $\alpha\beta$ interface. On the other hand if the interface lies in the lip found in a complete-wetting profile (so $\tilde{m}_1 > m^X > m_\beta$) then the interface remains bound close to the wall in the wetting limit. In order to derive an interface model which correctly recovers known behaviour near the wall and unbinding interface simultaneously we are led to introduce a two-field interface Hamiltonian

$$\mathcal{H}^{(2)}[l_1, l_2] = \int \mathrm{d}\boldsymbol{y}\, \{\tfrac{1}{2}\boldsymbol{\Sigma}_{\mu\nu}(l_1, l_2)(\nabla l_\mu)\cdot(\nabla l_\nu) + W_2(l_1, l_2)\} \tag{10}$$

where $\mu, \nu = 1, 2$ and a summation is implied by a repeated suffix. Here we assume l_1 and l_2 are surfaces of fixed magnetization m_1^X and m_2^X respectively, with typically $m_1^X \approx \tilde{m}_1$ and $m_2^X = 0$. Note that in the coupled theory the stiffness coefficient is replaced by a stiffness matrix $\boldsymbol{\Sigma}(l_1, l_2)$ while the binding potential W_2 has two contributions, $W_2(l_1, l_2) = U(l_1) + W(l_2 - l_1)$, where W is similar in form to the capillary wave binding potential. The additional term $U(l_1)$ simply acts to bind the lower surface to the wall and may safely be expanded about its minimum value $l_0 \approx 0$, thus $U(l_1) \approx r_0 l_1^2/2$.

Formally one may exactly derive the two-point structure factor $G(z_1, z_2; Q)$ from the two-field model with $m_1^X = \tilde{m}(z_1)$ and $m_2^X = \tilde{m}(z_2)$ [14] while for n-point correlation functions one should consider an n-field interface model. However, we stress that there are only two distinct behaviours for surfaces of fixed magnetization and so the two-field model (10) is sufficient at a qualitative level. Furthermore, for the fluctuation behaviour discussed in the following sections the inclusion of further fields has no significant effect and so from here on we restrict our attention to two-field models.

2.3. Renormalization of the capillary parameter

The inclusion of an extra field in the effective Hamiltonian model is also found to have an impact on the predictions for critical behaviour near complete wetting in three dimensions. This is most clearly observed in the critical amplitude describing the average thickness of the adsorbed layer $\langle l \rangle$. Specifically we define the dimensionless adsorption amplitude

$$\theta = \lim_{h \to 0-} \left[\frac{\kappa \langle l \rangle}{\ln |h|^{-1}} \right] \tag{11}$$

where recall the limit $h \to 0-$ describes the approach to complete wetting. At MF level $\theta = 1$, while when fluctuation effects are included via an RG treatment of the capillary wave model one finds that θ depends explicitly on the capillary parameter ω given by (7). In particular [5]

$$\theta = \begin{cases} 1 + \omega/2 & 0 < \omega < 2 \\ \sqrt{2\omega} & \omega > 2. \end{cases} \tag{12}$$

Calculations based upon a simple cubic Ising model estimate $\omega \approx 0.8$ in the range $0.6T_c$–T_c decreasing for smaller values of temperature [17], and hence provided we are sufficiently above the wetting temperature the capillary wave model predicts $\theta \approx 1.4$.

In order to determine the effect of including a second field in the interface model it is necessary to repeat the RG calculation for the two-field model. This has been done in the case where the position dependence of the stiffness coefficients is ignored and the two-field binding potential is expanded as described in section 2.2. Hence the capillary wave model (1) is replaced by

$$\mathcal{H}^{(2)}[l_1, l_2] = \int \mathrm{d}\boldsymbol{y}\, \{\tfrac{1}{2}\Sigma_{\alpha\beta}(\nabla l_2)^2 + \tfrac{1}{2}\tilde{\Sigma}_{w\beta}(\nabla l_1)^2 + \tfrac{1}{2}r_0 l_1^2 + W(l_2 - l_1)\} \qquad (13)$$

where $\tilde{\Sigma}_{w\beta} = \Sigma_{w\beta} - \phi_1(\tilde{m}_1)$ is the stiffness of the wall–β-phase interface. In this case the critical behaviour is determined from the renormalized binding potential, and hence we must compare the RG flow of $W(l_2 - l_1)$ with the flow of $W(l)$ in the capillary wave model. To this end it is sufficient to concentrate on the RG flow equations for the appropriate binding potentials[5].

Here we consider a simple linear functional RG applied in three dimensions and skip the mathematical details, which can be found elsewhere (see e.g. [6, 18]). If we let t denote the renormalization parameter then for the capillary wave model the binding potential flow is given by

$$\left[-\frac{\partial}{\partial t} + 2 + \omega\frac{\partial^2}{\partial l^2}\right] W^{(t)}(l) = 0 \qquad (14)$$

where the presence of the capillary parameter in the flow equation directly yields the ω-dependence of the critical amplitude θ. Repeating the analysis for the two-field model gives

$$\left[-\frac{\partial}{\partial t} + 2 + (\omega + \omega_1)\frac{\partial^2}{\partial \Delta l^2}\right] W^{(t)}(\Delta l) = 0 \qquad (15)$$

where $\Delta l \equiv l_2 - l_1$ and where we define

$$\omega_1 = \frac{k_{\mathrm{B}}T\kappa^2}{4\pi(\tilde{\Sigma}_{w\beta} + r_0/\Lambda_1^2)} \qquad (16)$$

in analogy with (7), with Λ_1 the implicit momentum cutoff of the lower field l_1. Comparing (14) and (15) reveals that the only effect of including the second field is an effective renormalization of the capillary parameter with $\omega \to \omega_{\mathrm{eff}} = \omega + \omega_1$. Inclusion of additional fields does not further renormalize the capillary parameter since one finds including two or more fields representing surfaces of fixed magnetization which display the same behaviour at the transition gives the same contribution as a single field of that type, and as discussed earlier there are only two distinct types of behaviour for surfaces of fixed magnetization.

The contribution ω_1 has been estimated [18] and is found to be $\omega_1 \approx 0.7$ so that $\omega_{\mathrm{eff}} \approx 1.5$. The two-field model result for the adsorption amplitude θ is simply (12) with ω replaced by ω_{eff} and hence this model predicts $\theta \approx 1.75$. Interestingly this amplitude has been independently determined by Binder *et al* using Monte Carlo simulations of finite-size effects in a three-dimensional Ising model [19]. Their results indicate that for temperatures deep into the complete-wetting regime $\theta = 1.72 \pm 0.1$, which cannot be accounted for by MF theory or the capillary wave model but which is consistent with the two-field prediction above.

We comment that the renormalization of the capillary parameter which is central to this result has also been shown in nonlinear RG studies where the position dependence of the stiffness coefficients has again been ignored [20], and in Monte Carlo simulations of a discrete version of the interface model [21]. Hence both critical amplitude analyses and correlation function studies give strong support for the two-field model (10).

[5] An alternative approach is to directly examine the solutions $W^{(t)}(l)$ which are found upon integrating the flow equations. The same conclusions are found in both cases and so for convenience we choose the flow equations as our point of reference in this paper.

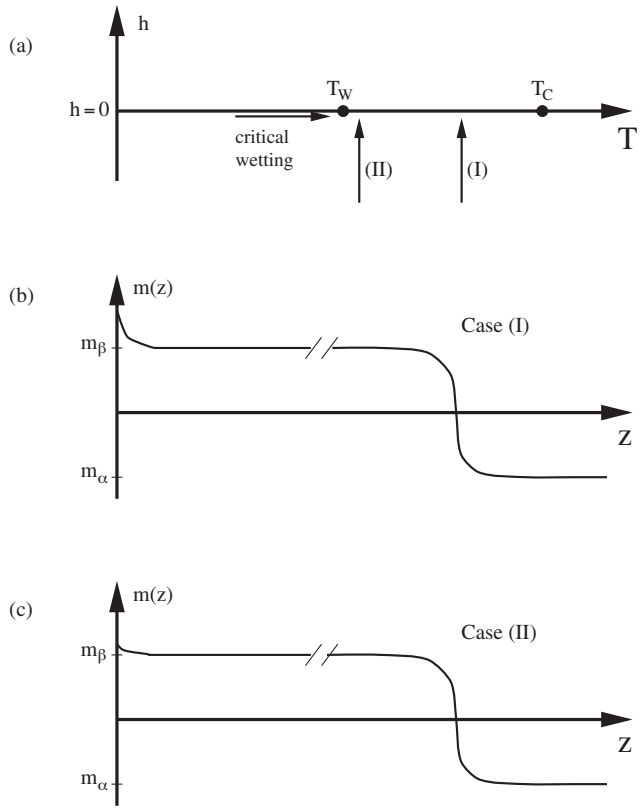

Figure 1. (*a*) Schematic wetting phase diagram highlighting the approach to critical wetting and two routes to complete wetting (bulk field $h \to 0$), the first (I) for temperature T well above T_W and the second (II) close to T_W. The corresponding order parameter profiles $m(z)$ are shown in (*b*) and (*c*). Note that the profile flattens at the wall as we approach the wetting temperature.

2.4. Proper collective coordinates

While the simple two-field theory discussed above has proven successful in describing complete wetting well above the wetting temperature, problems arise in applying the model close to T_W or for critical wetting. These problems are directly associated with the momentum cutoff of the lower field Λ_1. The standard interpretation of interface models dictates that the use of an interfacial-like collective coordinate is only valid if the cutoff $\Lambda_1 \ll \sqrt{\tilde{\Sigma}_{w\beta}/k_B T}$ [1, 22]. Within a piecewise parabolic approximation for the free-energy density $\Phi(m)$, the surface tension is found to vanish near T_W as $\tilde{\Sigma}_{w\beta} \sim (T - T_W)^2$ [3]. Indeed this result remains valid providing one may locally expand $\Phi(m)$ around m_β in a parabolic fashion. In these cases we can associate the vanishing of the surface tension with the flattening of the order parameter wetting profile at the wall near T_W (see figure 1). From quite general graphical construction arguments, the approach to the critical wetting temperature T_W involves a flattening of the order parameter profile at the wall with $m_1 \to m_\beta$ and $m_1' \to 0$ as $T \to T_W$ (see [5, 23]). In particular $m_1' \sim (T - T_W)$ so that, within a parabolic approximation at least, $\tilde{\Sigma}_{w\beta} \sim {m_1'}^2$. We interpret this result as indicative of a decoupling occurring between fluctuations of the unbinding interface and those at the wall near the wetting temperature. However, the two-field

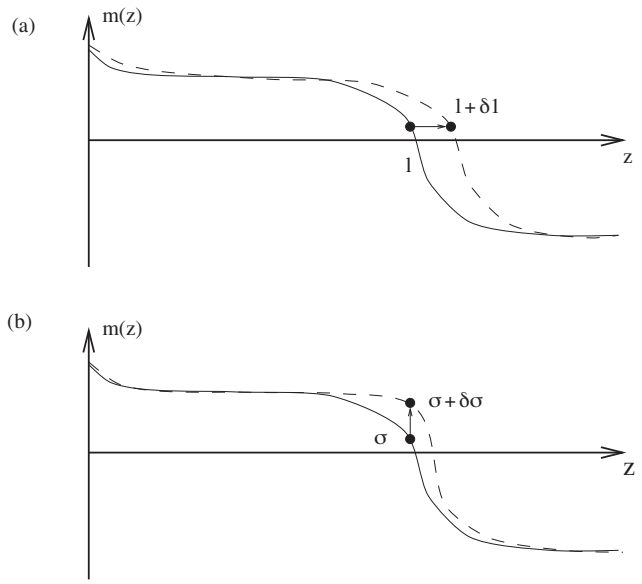

Figure 2. Schematic representation of the effect upon the constrained order-parameter profile $m(z)$ of pertubations of (a) an interfacial-like collective coordinate $l \to l + \delta l$, and (b) a spin-like collective coordinate $\sigma \to \sigma + \delta\sigma$.

model (10) is insufficient to quantitatively describe the crossover from complete to critical wetting-like behaviour because of the vanishing of Λ_1.

This problem has been elegantly resolved by Parry and Swain [3], who recognized that the correlation function structure described in section 2.2 may be recovered using a generalized two-field model

$$\mathcal{H}^{(2)}[X_1, X_2] = \int \mathrm{d}\boldsymbol{y}\, \{\tfrac{1}{2}\boldsymbol{\Sigma}_{\mu\nu}(X_1, X_2)(\nabla X_\mu)\cdot(\nabla X_\nu) + W_2(X_1, X_2)\} \qquad (17)$$

where $X_1(\boldsymbol{y})$ and $X_2(\boldsymbol{y})$ are some choice of collective coordinates representing order-parameter fluctuations near the wall and unbinding interface respectively. The interfacial choice $l(\boldsymbol{y})$ is one option; a 'spin-like' collective coordinate $\sigma(\boldsymbol{y})$ implemented by constraining the order-parameter profile to satisfy $m(\boldsymbol{y}, z^X) = \sigma(\boldsymbol{y})$ for some fixed z^X would be another. The reason for describing the collective coordinates as interfacial-like (l) or spin-like (σ) is clarified in figure 2, where we schematically sketch the effect of varying l or σ on the constrained order-parameter profile. Varying the value of l essentially shifts the location of the interface (figure 2(a)), and hence we identify l with the interface location. Varying σ distorts the shape of the interface via the enhancement of the profile in a vertical direction (figure 2(b)). Since this corresponds to a local perturbation in the average value of the magnetization we associate this coordinate with a local variation in the spins. In general the $X_i(\boldsymbol{y})$ in (17) will be composed of some combination of the two using an angle δ to describe the relative contributions of the interfacial- and spin-like components, where $\delta = \pi/2$ corresponds to an interfacial-like coordinate and $\delta = 0$ corresponds to a spin-like one (see figure 3). Coordinates parametrized in this way have been termed proper collective coordinates, and the problem answered by Parry and Swain was to determine which is the 'optimal' choice of angle for a given collective coordinate. This is determined by selecting the angle which yields the most accurate Gaussian approximation for fluctuations [3] and corresponds to the direction normal

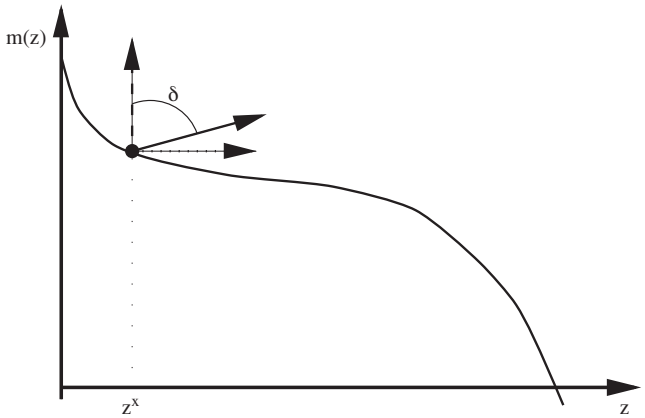

Figure 3. Schematic representation of the angle δ which determines the character of a collective coordinate defined at position z^X. The dashed line (corresponding to $\delta = 0$) represents a spin-like choice, while the dotted line ($\delta = \pi/2$) represents a purely interfacial-like collective coordinate.

to the order parameter profile. This can be understood intuitively as the choice which accesses the largest region of magnetization phase space for a fluctuation of given magnitude.

The conclusion of this paper is that the interfacial-like coordinate $l_2(\boldsymbol{y})$ is a suitable choice for the upper field for both complete and critical wetting, while the lower field $X_1(\boldsymbol{y})$ changes continuously from an interfacial- to a spin-like coordinate as the temperature is decreased towards T_W. With this optimal choice the relevant stiffness component Σ_{11} in (17) is always finite and so the problems associated with a vanishing momentum cutoff no longer arise.

2.5. Summary

In summary, recent advances have shown that it is appropriate to replace the capillary wave model by a two-field model which includes a description of order-parameter fluctuations near the wall. Furthermore a generalized choice of collective coordinate will be necessary in order to describe both complete and critical wetting adequately. Finally the work of FJ demonstrates that the relevant stiffness coefficients in (17) should contain a weak dependence on the collective coordinates, which may have an important effect on critical behaviour. To date this coordinate dependence has been largely ignored, for example in the studies of the renormalized capillary parameter, and it is the aim of this paper to establish the role it plays using a suitably extended RG approach.

3. Nonlinear renormalization group analysis

In this section we derive a nonlinear functional RG scheme suitable for dealing with a generalized two-field effective Hamiltonian such as (17). For convenience we redefine our initial bare Hamiltonian here as

$$\mathcal{H}^{(2)}[X_1, X_2] = \int^{\Lambda} \mathrm{d}\boldsymbol{y}\, \{\tfrac{1}{2}\Sigma_1(X_1, X_2)(\nabla X_1)^2 + \Sigma_3(X_1, X_2)(\nabla X_1)\cdot(\nabla X_2) + \tfrac{1}{2}\Sigma_2(X_1, X_2)(\nabla X_2)^2 + W(X_1, X_2)\} \tag{18}$$

where the $X_i(\boldsymbol{y})$ are the generalized coordinates discussed in the last section and we have explicitly highlighted the dependence on a momentum cutoff Λ, which we may assume is the

same for both proper collective coordinates and is essentially the same cutoff used in the simple capillary wave model [3]. We further separate out the position-dependent contributions to the stiffness coefficients by writing

$$\Sigma_i(X_1, X_2) = \Sigma_{i\infty} + \Delta\Sigma_i(X_1, X_2) \qquad i = 1, 2, 3. \tag{19}$$

The constant contribution $\Sigma_{i\infty}$ may be identified as follows: for each collective coordinate $X_j(\boldsymbol{y})$ there is a corresponding surface $Z_j(\boldsymbol{y})$ at which the appropriate constraint is defined, $\Sigma_{i\infty}$ is then given by the limit of $\Sigma(X_1, X_2)$ as $Z_1 \to 0$ and $Z_2 \to \infty$.

The RG procedure consists of performing a partial trace in the partition function over small-scale fluctuations, $X_i^>(\boldsymbol{y})$ $(i = 1, 2)$ say, with wavenumbers in the range $\Lambda/b < |\boldsymbol{k}| < \Lambda$ where $b > 1$ is an arbitrary rescaling factor. The partial trace over $X_1^>(\boldsymbol{y})$ and $X_2^>(\boldsymbol{y})$ yields a new, intermediate Hamiltonian with momentum cutoff Λ/b. We must then make the scale transformation appropriate for RG studies of unbinding transitions [11]

$$\boldsymbol{y} \to \boldsymbol{y}' = \boldsymbol{y}/b \qquad X_i \to X_i' = X_i/b^{\zeta} \qquad (i = 1, 2) \tag{20}$$

where $\zeta = (3 - d)/2$ is the roughness exponent. This rescaling ensures that the momentum cutoff of the intermediate Hamiltonian is returned to its original value allowing the process to be repeated iteratively.

In general the trace over short-wavelength fluctuations described above cannot be performed exactly and hence some form of approximation must be introduced. Here we use an extension of the Wilson scheme developed by Lipowsky and Fisher [11], which has proved valuable in studying unbinding behaviour. This scheme is based around the assumption that the $X_i^>(\boldsymbol{y})$ can be expanded in terms of a complete set of eigenfunctions which are localized both in real and momentum space (for an instructive account of this technique see [24]), and has the advantage that by construction it is *exact* at linear order. Traditionally this scheme has not allowed for the inclusion of position-dependent stiffness coefficients; however, this problem has recently been overcome for single-field interface models with a position-dependent stiffness [9]. Here we extend that work for our two-field model (18) further incorporating generalized coordinates. This can be achieved without including any additional approximations in the RG scheme and hence rather than repeating the technical details of the scheme here we refer interested readers to [9] for a detailed description of the relevant approximations.

3.1. Recursion relations and flow equations

In this subsection we detail the key results found from applying the RG method outlined above. In particular we begin with the recursion relations which describe how the binding potential and stiffness coefficients are renormalized under the scheme. To this end we note that the initial potential $W^{(0)}(l_1, l_2) \equiv W(l_1, l_2)$ and position-dependent stiffness contributions $\Delta\Sigma_i^{(0)}(l_1, l_2) \equiv \Delta\Sigma_i(l_1, l_2)$ $(i = 1, 2, 3)$ are renormalized via successive applications of

$$W^{(N+1)}(l_1, l_2) = \mathcal{R}_W[W^{(N)}(l_1, l_2), \Delta\Sigma_1^{(N)}(l_1, l_2), \Delta\Sigma_2^{(N)}(l_1, l_2), \Delta\Sigma_3^{(N)}(l_1, l_2)] \tag{21}$$

and

$$\Delta\Sigma_i^{(N+1)}(l_1, l_2) = \mathcal{R}_{\Delta\Sigma_i}[W^{(N)}(l_1, l_2), \Delta\Sigma_1^{(N)}(l_1, l_2), \Delta\Sigma_2^{(N)}(l_1, l_2), \Delta\Sigma_3^{(N)}(l_1, l_2)] \qquad i = 1, 2, 3. \tag{22}$$

Before defining the precise form of these recursion operators it is convenient to introduce the following functions:

$$g(x_1, x_1'; x_2, x_2') = W(x_1 + x_1', x_2 + x_2') + W(x_1 - x_1', x_2 - x_2') \tag{23}$$

$$f_i(x_1, x_1'; x_2, x_2') = \Delta\Sigma_i(x_1 + x_1', x_2 + x_2') + \Delta\Sigma_i(x_1 - x_1', x_2 - x_2') \tag{24}$$

where the latter equation is valid for $i = 1, 2, 3$. Finally we define

$$E(x_1, x_1'; x_2, x_2') = \exp\left\{ -\frac{1}{2}\sum_{i=1}^{2}\left[1 + \frac{f_i(b^\zeta x_1, x_1'; b^\zeta x_2, x_2')}{2\Sigma_{i\infty}}\right]\left(\frac{x_i'}{\tilde{a}_i}\right)^2 \right.$$
$$\left. -\left[1 + \frac{f_3(b^\zeta x_1, x_1'; b^\zeta x_2, x_2')}{2\Sigma_{3\infty}}\right]\left(\frac{x_1'x_2'}{\tilde{a}_3^2}\right) - \frac{1}{2\tilde{\nu}}g(b^\zeta x_1, x_1'; b^\zeta x_2, x_2')\right\} \tag{25}$$

where

$$\tilde{\nu} = \tilde{\nu}(b) = k_{\mathrm{B}}T\int_{\Lambda/b}^{\Lambda}\frac{d^{d-1}k}{(2\pi)^{d-1}} \tag{26}$$

and the $\tilde{a}_i^2$ are 'arbitrary' lengthscales. More precisely there is a single arbitrary lengthscale because one finds that the $\tilde{a}_i^2$ are related via $\Sigma_{1\infty}\tilde{a}_1^2 = \Sigma_{2\infty}\tilde{a}_2^2 = \Sigma_{3\infty}\tilde{a}_3^2$ and, as we shall show later, this lengthscale can be fixed by demanding that the RG procedure should be exact at linear order, yielding

$$\tilde{a}_i^2 = \tilde{a}_i^2(b) = \frac{k_{\mathrm{B}}T}{\Sigma_{i\infty}}\int_{\Lambda/b}^{\Lambda}\frac{d^{d-1}k}{k^2(2\pi)^{d-1}} \qquad i = 1, 2, 3. \tag{27}$$

Using these definitions the recursion operators are simply defined as

$$\mathcal{R}_W \equiv -\tilde{\nu}b^{d-1}\ln\left[\int_{-\infty}^{\infty}\int_{-\infty}^{\infty}\frac{\mathrm{d}X_1'\mathrm{d}X_2'}{2\pi\tilde{a}_1\tilde{a}_2}\sqrt{\left(1 - \frac{{\Sigma_{3\infty}}^2}{\Sigma_{1\infty}\Sigma_{2\infty}}\right)}E(X_1, X_1'; X_2, X_2')\right] \tag{28}$$

and

$$\mathcal{R}_{\Delta\Sigma_i} \equiv \frac{\int_{-\infty}^{\infty}\int_{-\infty}^{\infty}\mathrm{d}X_1'\,\mathrm{d}X_2'\,f_i(b^\zeta X_1, X_1'; b^\zeta X_2, X_2')E(X_1, X_1'; X_2, X_2')}{2\int_{-\infty}^{\infty}\int_{-\infty}^{\infty}\mathrm{d}X_1''\,\mathrm{d}X_2''\,E(X_1, X_1''; X_2, X_2'')} \tag{29}$$

for $i = 1, 2, 3$.

These recursion relations are an effective starting point for numerical studies of the RG flow where (21) and (22) may be solved repeatedly for fixed $b > 1$, in an analogous manner to previous single-field studies [9, 11]. However, for analytic studies the recursion operators are somewhat unwieldy and it is often preferable to study the flow equations resulting from considering the infinitesimal rescaling limit $b = \mathrm{e}^t, t \to 0$. Applying this limit to the equations above yields the following coupled flow equations:

$$\frac{\partial W}{\partial t} = (d-1)W + \zeta X_1\frac{\partial W}{\partial X_1} + \zeta X_2\frac{\partial W}{\partial X_2}$$
$$+\Omega(d)\ln\left[\frac{(\frac{\partial^2 W}{\partial X_1^2} + \Lambda^2\Sigma_1)(\frac{\partial^2 W}{\partial X_2^2} + \Lambda^2\Sigma_2) - (\frac{\partial^2 W}{\partial X_1\partial X_2} + \Lambda^2\Sigma_3)^2}{(\Sigma_{1\infty}\Sigma_{2\infty} - {\Sigma_{3\infty}}^2)\Lambda^4}\right] \tag{30}$$

and

$$\frac{\partial \Sigma_i}{\partial t} = \zeta X_1\frac{\partial \Sigma_i}{\partial X_1} + \zeta X_2\frac{\partial \Sigma_i}{\partial X_2} + \Omega(d)$$
$$\times\left[\frac{(\frac{\partial^2 W}{\partial X_1^2} + \Lambda^2\Sigma_1)\frac{\partial^2\Sigma_i}{\partial X_2^2} + (\frac{\partial^2 W}{\partial X_2^2} + \Lambda^2\Sigma_2)\frac{\partial^2\Sigma_i}{\partial X_1^2} - 2(\frac{\partial^2 W}{\partial X_1\partial X_2} + \Lambda^2\Sigma_3)\frac{\partial^2\Sigma_i}{\partial X_1\partial X_2}}{(\frac{\partial^2 W}{\partial X_1^2} + \Lambda^2\Sigma_1)(\frac{\partial^2 W}{\partial X_2^2} + \Lambda^2\Sigma_2) - (\frac{\partial^2 W}{\partial X_1\partial X_2} + \Lambda^2\Sigma_3)^2}\right] \tag{31}$$

for $i = 1, 2, 3$, and where $\Omega(d) = k_{\mathrm{B}}T\Lambda^{d-1}/[(4\pi)^{(\frac{d-1}{2})}\Gamma(\frac{d-1}{2})]$.

An intriguing feature of these equations is that it is the full stiffnesses $\Sigma_i(X_1, X_2)$ which are involved rather than just the position-dependent contributions $\Delta\Sigma_i(X_1, X_2)$. This has not been

observed in previous studies simply because the effect is only apparent at quadratic order or above in the stiffnesses, and has therefore not been accessible in the earlier linear RG analyses which have been applied to analyse the effect of position-dependent stiffness contributions. However the division embodied in (19) is primarily employed as a mathematical aid to apply the RG and it seems appropriate that the governing equations for the RG flow should depend on the full stiffness contributions. Finally in this subsection we observe that the flow equations may be cast into a convenient matrix form. To this end we explicitly write the stiffness matrix

$$\boldsymbol{\Sigma}(X_1, X_2) = \begin{pmatrix} \Sigma_1(X_1, X_2) & \Sigma_3(X_1, X_2) \\ \Sigma_3(X_1, X_2) & \Sigma_2(X_1, X_2) \end{pmatrix} \tag{32}$$

and define

$$\boldsymbol{U} = \begin{pmatrix} \frac{\partial^2 W}{\partial X_1^2} + \Lambda^2 \Sigma_1 & \frac{\partial^2 W}{\partial X_1 \partial X_2} + \Lambda^2 \Sigma_3 \\ \frac{\partial^2 W}{\partial X_1 \partial X_2} + \Lambda^2 \Sigma_3 & \frac{\partial^2 W}{\partial X_2^2} + \Lambda^2 \Sigma_2 \end{pmatrix} \qquad \boldsymbol{U}_\infty = \Lambda^2 \begin{pmatrix} \Sigma_{1\infty} & \Sigma_{3\infty} \\ \Sigma_{3\infty} & \Sigma_{2\infty} \end{pmatrix}. \tag{33}$$

In addition we define a vector operator

$$\hat{\boldsymbol{\delta}} = \begin{pmatrix} \frac{\partial}{\partial X_2} \\ -\frac{\partial}{\partial X_1} \end{pmatrix}. \tag{34}$$

With these definitions in place the flow equations (30) and (31) may be written as

$$\frac{\partial W}{\partial t} = (d-1)W + \zeta X_1 \frac{\partial W}{\partial X_1} + \zeta X_2 \frac{\partial W}{\partial X_2} + \Omega(d) \ln \left[\frac{\det \boldsymbol{U}}{\det \boldsymbol{U}_\infty} \right] \tag{35}$$

and

$$\frac{\partial \boldsymbol{\Sigma}}{\partial t} = \left\{ \zeta X_1 \frac{\partial}{\partial X_1} + \zeta X_2 \frac{\partial}{\partial X_2} + \frac{\Omega(d)}{(\det \boldsymbol{U})} (\boldsymbol{U} \hat{\boldsymbol{\delta}})^T \hat{\boldsymbol{\delta}} \right\} \boldsymbol{\Sigma}. \tag{36}$$

While this formulation does not add any further physical insight to the relevant importance of the various terms it does provide a particularly compact presentation, and should be considered the main result of this section.

3.2. Limiting cases

In this section we check our RG scheme recovers known results in some special limiting cases. First we note that in the limit $\Sigma_{1\infty} \to \infty$ the fluctuations of the lower surface are completely suppressed. As a result the only fluctuating field is X_2, and the two remaining functions W and Σ_2 depend only on X_2. Further, in this limit the flow equations above reduce to

$$\frac{\partial W}{\partial t} = (d-1)W + \zeta X_2 \frac{\partial W}{\partial X_2} + \Omega(d) \ln \left[1 + \frac{1}{\Lambda^2 \Sigma_{2\infty}} \left\{ \frac{\partial^2 W}{\partial X_2^2} + \Lambda^2 \Delta \Sigma_2 \right\} \right] \tag{37}$$

and

$$\frac{\partial \Sigma_2}{\partial t} = \zeta X_2 \frac{\partial \Sigma_2}{\partial X_2} + \frac{\Omega(d)}{\Lambda^2 \Sigma_{2\infty}} \frac{\partial^2 \Sigma_2}{\partial X_2^2} \left[1 + \frac{1}{\Lambda^2 \Sigma_{2\infty}} \left\{ \frac{\partial^2 W}{\partial X_2^2} + \Lambda^2 \Delta \Sigma_2 \right\} \right]^{-1} \tag{38}$$

which precisely recovers the single-field Hamiltonian results found in previous studies [9].

Finally we confirm that the nonlinear scheme described above is exact to leading order in both the binding potential and position-dependent stiffness contributions. As a simple demonstration we consider the special case where $\Sigma_{3\infty} = 0$ and $\Delta \Sigma_i \equiv 0 \ \forall i$. In this case we simply have a recursion relation for the binding potential $W(X_1, X_2)$, which we expand to linear order to find

$$W^{(b)}(X_1, X_2) = b^{d-1} \int_{-\infty}^{\infty} \int_{-\infty}^{\infty} \frac{\mathrm{d}X_1' \, \mathrm{d}X_2'}{2\pi \tilde{a}_1 \tilde{a}_2} W^{(0)}(X_1', X_2') \exp \left\{ -\frac{1}{2} \sum_{i=1}^{2} \left(\frac{b^\zeta X_i - X_i'}{\tilde{a}_i} \right)^2 \right\}. \tag{39}$$

This equation is in perfect agreement with the exact linear functional RG result for the binding potential provided we make the identification (27) for $\tilde{a}_i^2$ [18]. We can repeat this exercise without making any special choice for the stiffnesses and again precisely recover the corresponding linear RG recursion relations; however, we omit the details here for brevity. Instead we concentrate on the corresponding linear flow equations, which, from (35) and (36), can be read off as

$$\frac{\partial W}{\partial t} = (d-1)W + \zeta X_1 \frac{\partial W}{\partial X_1} + \zeta X_2 \frac{\partial W}{\partial X_2} + \tilde{A}_1^2 \left(\frac{\partial^2 W}{\partial X_2^2} + \Lambda^2 \Delta\Sigma_2 \right) + \tilde{A}_2^2 \left(\frac{\partial^2 W}{\partial X_1^2} + \Lambda^2 \Delta\Sigma_1 \right) - 2\tilde{A}_3^2 \left(\frac{\partial^2 W}{\partial X_1 \partial X_2} + \Lambda^2 \Delta\Sigma_3 \right) \tag{40}$$

and

$$\frac{\partial \Delta\Sigma_i}{\partial t} = \zeta X_1 \frac{\partial \Delta\Sigma_i}{\partial X_1} + \zeta X_2 \frac{\partial \Delta\Sigma_i}{\partial X_2} + \tilde{A}_1^2 \frac{\partial^2 \Delta\Sigma_i}{\partial X_2^2} + \tilde{A}_2^2 \frac{\partial^2 \Delta\Sigma_i}{\partial X_1^2} - 2\tilde{A}_3^2 \frac{\partial^2 \Delta\Sigma_i}{\partial X_1 \partial X_2} \qquad i = 1, 2, 3 \tag{41}$$

and where the $\tilde{A}_i^2$ are defined as

$$\tilde{A}_i^2 = \frac{k_B T \Lambda^{d-3}}{(4\pi)^{\frac{d-1}{2}} \Gamma(\frac{d-1}{2})} \frac{\Sigma_{i\infty}}{(\Sigma_{1\infty}\Sigma_{2\infty} - \Sigma_{3\infty}{}^2)} \qquad i = 1, 2, 3. \tag{42}$$

Once again these results are fully consistent with earlier linear RG analyses [18] providing further support for the nonlinear RG scheme employed in this section.

In conclusion we have described a nonlinear functional RG scheme which for the first time allows the study of two-field effective models which include position-dependent stiffness contributions. The main results are compactly embodied in the flow equations (35) and (36). We have confirmed that this scheme recovers known single-field results in the appropriate limit and that it is exact at linear order. We further observe that if the position dependence of the stiffness coefficients is ignored the flow equations correctly reduce to those found in simpler two-field nonlinear RG analyses where the position-dependent stiffnesses were excluded [20]. Hence in conclusion we believe there is compelling evidence that our scheme is generally applicable to the two-field model (18).

4. Applications to complete and critical wetting

Motivated by the RG analysis of the last section we now look to address some of the outstanding issues in the study of complete and critical wetting. Firstly we ask how the inclusion of position-dependent stiffness coefficients affects the renormalization of the capillary parameter near complete wetting discussed in section 2.3. Later we investigate the impact of including multiple fields on the prediction of fluctuation-induced first-order transitions at critical wetting.

4.1. Renormalization of the capillary parameter revisited

The goal of this subsection is to apply the RG scheme to determine how the position-dependent contributions to the stiffness enter the renormalization of the capillary parameter, and what effect these changes will have for predictions of critical behaviour. Thus we restrict our attention to the marginal dimensionality $d = 3$ and consider temperatures deep in the complete-wetting regime, where the effect of the capillary parameter renormalization is most pronounced. For this choice we know from section 2.4 that we may safely identify both collective coordinates

as interfacial-like, $X_i(\boldsymbol{y}) \equiv l_i(\boldsymbol{y})$ $i = 1, 2$. In order to gain some insight into how the position-dependent stiffnesses enter the capillary parameter renormalization we start by examining the simplest generalization of (13) that includes some position dependence. Namely,

$$\mathcal{H}^{(2)}[l_1, l_2] = \int \mathrm{d}\boldsymbol{y}\, \{\tfrac{1}{2}\Sigma_2(l_2 - l_1)(\nabla l_2)^2 + \tfrac{1}{2}\tilde{\Sigma}_{w\beta}(\nabla l_1)^2 + \tfrac{1}{2}r_0 l_1^2 + W(l_2 - l_1)\} \tag{43}$$

where $\Sigma_2(l) = \Sigma_{\alpha\beta} + \Delta\Sigma_2(l)$ and $\Delta\Sigma_2(l) \to 0$ as $l \to \infty$. This choice is motivated by explicit calculations of the stiffness matrix elements which show that, provided the field l_1 is located close to the wall, the stiffnesses only depend on the relative distance $l_2 - l_1$ [14]. Furthermore, since the leading contribution to the effective capillary parameter arises from the upper field l_2 it seems reasonable to assume that only including position dependence in Σ_2 will provide a plausible guide to the importance of including position dependence for the minimum mathematical effort. We address the issue of what happens if (43) is replaced by a model including the full position dependence of stiffness coefficients, including the cross-term $\Sigma_3(l_2 - l_1)(\nabla l_1) \cdot (\nabla l_2)$, at the end of this subsection.

Following the discussion in section 2 we will use the RG flow equations to indicate the renormalization of the capillary parameter. With this in mind we first clarify how the capillary parameter ω may be identified in the nonlinear flow equations for a single-field model with a position-dependent stiffness coefficient. In this case we have two coupled equations, one for the binding potential $W(l)$ and one for the position-dependent stiffness contribution $\Sigma(l)$. The appropriate equations can be read off from (37) and (38) to be

$$\frac{\partial W^{(t)}(l)}{\partial t} = 2W^{(t)}(l) + \frac{k_{\mathrm{B}}T\Lambda^2}{4\pi}\ln\left[\frac{\Sigma^{(t)}(l)}{\Sigma_{\alpha\beta}} + \frac{4\pi\omega}{k_{\mathrm{B}}T\Lambda^2}\frac{\partial^2 W^{(t)}(l)}{\partial l^2}\right] \tag{44}$$

and

$$\frac{\partial \Sigma^{(t)}(l)}{\partial t} = 4\pi\omega\frac{\partial^2\Sigma^{(t)}(l)}{\partial l^2}\left[\frac{\Sigma^{(t)}(l)}{\Sigma_{\alpha\beta}} + \frac{4\pi\omega}{k_{\mathrm{B}}T\Lambda^2}\frac{\partial^2 W^{(t)}(l)}{\partial l^2}\right]^{-1} \tag{45}$$

with ω given by (7), and where all lengths are measured in units of the bulk correlation length of the wetting phase. The remaining explicit dependence on $\Sigma_{\alpha\beta}$ essentially fixes an energy scale and can be removed by rescaling. For example, defining $S^{(t)}(l) \equiv \Sigma^{(t)}(l)/\Sigma_{\alpha\beta}$ results in equations for W and S analogous to (44) and (45) but with the $\Sigma_{\alpha\beta}$ dependence removed.

We can now compare with the results for our reduced two-field model (43). In this model we may treat the purely Gaussian term $\frac{1}{2}r_0 l_1^2$ exactly as has been done in previous studies [18, 22]. The final results can again be generally written in the compact form (35) and (36) but where the contribution $\Lambda^2\Sigma_{1\infty}$ in the first elements of the matrices $\boldsymbol{U}$ and $\boldsymbol{U}_\infty$ (see equation (33)) should be replaced by $(\Lambda^2\Sigma_{1\infty} + r_0)$. Including this modification yields the following coupled flow equations for the binding potential $W(l)$ and position-dependent stiffness contribution $\Sigma_2(l)$ where $l \equiv l_2 - l_1$:

$$\frac{\partial W^{(t)}(l)}{\partial t} = 2W^{(t)}(l) + \frac{k_{\mathrm{B}}T\Lambda^2}{4\pi}\ln\left[\frac{\Sigma_2^{(t)}(l)}{\Sigma_{\alpha\beta}} + \frac{4\pi}{k_{\mathrm{B}}T\Lambda^2}\left(\omega + \omega_1\frac{\Sigma_2^{(t)}(l)}{\Sigma_{\alpha\beta}}\right)\frac{\partial^2 W^{(t)}(l)}{\partial l^2}\right] \tag{46}$$

and

$$\begin{aligned}\frac{\partial \Sigma_2^{(t)}(l)}{\partial t} &= 4\pi\left(\omega + \omega_1\frac{\Sigma_2^{(t)}(l)}{\Sigma_{\alpha\beta}}\right)\frac{\partial^2\Sigma^{(t)}(l)}{\partial l^2} \\ &\quad\times\left[\frac{\Sigma_2^{(t)}(l)}{\Sigma_{\alpha\beta}} + \frac{4\pi}{k_{\mathrm{B}}T\Lambda^2}\left(\omega + \omega_1\frac{\Sigma_2^{(t)}(l)}{\Sigma_{\alpha\beta}}\right)\frac{\partial^2 W^{(t)}(l)}{\partial l^2}\right]^{-1}\end{aligned} \tag{47}$$

where ω_1 is given by (16). Comparing these last two flow equations with the preceding pair reveals that including the lower field l_1 leads to the capillary parameter ω being replaced by $\omega+\omega_1\Sigma_2^{(t)}(l)/\Sigma_{\alpha\beta}$. The nonlinear RG thus reveals an additional contribution $\omega_1\Delta\Sigma_2^{(t)}(l)/\Sigma_{\alpha\beta}$ not accessible in earlier linear analyses. By including nonlinear effects and position-dependent stiffness contributions we identify the *transient flow* of the effective capillary parameter as carried by the t-dependence in $\Sigma_2^{(t)}(l)$. However, the critical behaviour at complete wetting is determined purely by the fixed-point behaviour of the binding potential and stiffness and so we must address how these functions evolve under the RG flow.

Solving the flow equations analytically is beyond the scope of this paper, but we can obtain the information we need from a fixed-point study. Following the procedure described by Lipowsky [25] one can integrate proposed fixed-point solutions forward from small l looking for solutions which match with the known large-l behaviour, which can be determined from linearizing the flow equations. A limited number of fixed-point pairs, $W^*(l)$ and $\Sigma_2^*(l)$ say, are identified and in each case we find that $\Sigma_2^*(l)$ is constant $\forall l$. For large l we know $\Sigma_2(l)\to\Sigma_{\alpha\beta}$ from our definitions and so at the fixed points we must identify $\Sigma_2^*(l)\equiv\Sigma_{\alpha\beta}$. With this determined the fixed-point binding potential $W^*(l)$ is found to have the same form as determined in simple single-field studies but with the capillary parameter replaced by $\omega_{\rm eff}=\omega+\omega_1$. Hence although the transient form of the renormalized capillary parameter is modified by the inclusion of a position-dependent stiffness, the relevant results for critical behaviour are again only dependent on $\omega_{\rm eff}=\omega+\omega_1$ and so the results of earlier studies described in section 2.3 are fully supported by our analysis.

Given the results found above from including a position dependence in just the Σ_2 stiffness, one may anticipate that including position dependence in the other stiffness coefficients will not affect the ω-renormalization. We show that this is the case by considering a more general effective interface model. Thus in (43) we replace $\tilde\Sigma_{w\beta}$ by $\Sigma_1(l)=\tilde\Sigma_{w\beta}+\Delta\Sigma_1(l)$ and include a cross-term $\Sigma_3(l)(\nabla l_1)\cdot(\nabla l_2)$, where once again $l\equiv l_2-l_1$. We further note that in the limit of infinite separation $l\to\infty$ there is no interaction between the two interfaces and so quite generally $\Sigma_3(l)\to 0$ as $l\to\infty$. For this model a slightly more involved calculation again reveals a capillary parameter renormalization where in the RG flow equations

$$\omega\to\omega_{\rm eff}^{(t)}=\frac{k_{\rm B}T\Lambda^2}{4\pi}\left[\frac{(\Lambda^2\Sigma_1^{(t)}+r_0)+\Lambda^2\Sigma_2^{(t)}-2\Lambda^2\Sigma_3^{(t)}}{(\Lambda^2\tilde\Sigma_{w\beta}+r_0)\Lambda^2\Sigma_{\alpha\beta}}\right]$$
$$=\omega\left[\frac{(\Lambda^2\Sigma_1^{(t)}+r_0)-\Lambda^2\,\Sigma_3^{(t)}}{\Lambda^2\tilde\Sigma_{w\beta}+r_0}\right]+\omega_1\left[\frac{\Sigma_2^{(t)}-\Sigma_3^{(t)}}{\Sigma_{\alpha\beta}}\right]. \qquad (48)$$

Once again it is only the fixed-point (i.e. $t\to\infty$) value of $\omega_{\rm eff}^{(t)}$ which is important for critical behaviour. Noting that $\Sigma_1^{(t)}(l)\to\tilde\Sigma_{w\beta}$, $\Sigma_2^{(t)}(l)\to\Sigma_{\alpha\beta}$ and $\Sigma_3^{(t)}(l)\to 0$ for $t\to\infty$ shows that at the fixed point $\omega_{\rm eff}=\omega+\omega_1$. Hence as anticipated, in terms of critical behaviour, the capillary parameter renormalization is not affected by the inclusion of position-dependent stiffness coefficients.

4.2. Fluctuation-induced first-order transitions

The final topic we wish to study in this paper is the effect of including a second field in the interface model upon the FJ prediction of fluctuation-induced first-order transitions near critical wetting in three dimensions, as discussed in section 2.1. In particular we want to know whether this so-called stiffness instability mechanism is relevant in the two-field model, and if it is we wish to determine whether the effect is stronger, weaker or unchanged compared to the single-field predictions. This is particularly important since the mechanism is currently predicted to

be relevant in a region of parameter space (in particular a temperature range) whose border is close to the location where many of the simulation studies are performed [7, 8]. Hence any weakening of the predictions will greatly reduce the likelihood that this mechanism will play a role in interpreting future simulation results.

Since we are interested in the approach $T \to T_W$ we know from section 2.4 that the appropriate choice of collective coordinates for our two-field model is a spin-like coordinate near the wall $X_1(\boldsymbol{y}) = \sigma(\boldsymbol{y})$, and an interfacial coordinate at the unbinding interface $X_2(\boldsymbol{y}) = l(\boldsymbol{y})$. Hence we consider the Hamiltonian

$$\mathcal{H}^{(2)}[\sigma, l] = \int \mathrm{d}\boldsymbol{y}\, \{\tfrac{1}{2}\Sigma_1(\nabla\sigma)^2 + \tfrac{1}{2}\Sigma_2(\nabla l)^2 + \Sigma_3(\nabla\sigma)\cdot(\nabla l) + W(\sigma, l)\} \quad (49)$$

where quite generally $\Sigma_i = \Sigma_i(\sigma, l)$, $i = 1, 2, 3$. Recall that the stiffness instability mechanism was due to terms of $\mathcal{O}(l\mathrm{e}^{-2\kappa l})$ in the stiffness coefficient Σ_2 destabilizing the MF critical wetting transition. We further know from explicit calculations (see [3, 14] and later) that in the two-field theory the dominant position-dependent contribution to the stiffness matrix is $\mathcal{O}(l\mathrm{e}^{-\kappa l})$, which arises in Σ_3. To determine whether this order contribution is likely to be significant we first return to the nonlinear RG flow equations (30) and (31). Rather than attempting to numerically solve the system of four coupled nonlinear partial differential equations, which would require significant computational effort, we simply use the equations to try to gauge the relevant importance of the various stiffness contributions on the renormalized binding potential. To this end we consider the bare contribution to the expression (cf (30))

$$\left(\frac{\partial^2 W}{\partial\sigma^2} + \Lambda^2\Sigma_1\right)\left(\frac{\partial^2 W}{\partial l^2} + \Lambda^2\Sigma_2\right) - \left(\frac{\partial^2 W}{\partial\sigma\,\partial l} + \Lambda^2\Sigma_3\right)^2 \quad (50)$$

which appears in the flow equation for W, and compare this with the corresponding single-field contribution $\frac{\partial^2 W}{\partial l^2} + \Lambda^2\Sigma_2$. Evaluating (50) in a double-parabola approximation (see below for further details) we conclude that the lower stiffness Σ_1 does not contribute to the leading-order terms, while Σ_3 appears at least as important as Σ_2 and hence may significantly affect the stiffness instability mechanism. Clearly such observations are at best indicative of how the stiffnesses may enter the full analysis and are insufficient to provide quantitative or qualitative predictions.

To remedy this we provide a simple calculation based on a single-field effective interface model derived from (49) by tracing out the lower coordinate field σ. We start by evaluating the various terms in (49) using the reliable double-parabola approximation, which involves modelling the free-energy density $\Phi(m)$ in (2) by two parabolas [8, 26]. This calculation yields the stiffnesses and binding potential in terms of the planar constrained order-parameter profile $m_\pi(\sigma, l)$ as follows:

$$\Sigma_1(l) = \int_0^\infty \mathrm{d}z \left(\frac{\partial m_\pi}{\partial\sigma}\right)^2 = \frac{K}{2\kappa(1-\mathrm{e}^{-2\kappa l})^2}[(1-\mathrm{e}^{-4\kappa l}) - 4(\kappa l)\mathrm{e}^{-2\kappa l}] \quad (51)$$

$$\begin{aligned}\Sigma_2(\sigma, l) = \int_0^\infty \mathrm{d}z \left(\frac{\partial m_\pi}{\partial l}\right)^2 &= \Sigma_{\alpha\beta} - \frac{1}{2}K\kappa m_\beta^2 \\ &+ \frac{K\kappa[(1-\mathrm{e}^{-4\kappa l}) - 4(\kappa l)\mathrm{e}^{-2\kappa l}][m_\beta(1+\mathrm{e}^{-2\kappa l}) + 2(\sigma - m_\beta)\mathrm{e}^{-\kappa l}]^2}{2(1-\mathrm{e}^{-2\kappa l})^4}\end{aligned} \quad (52)$$

$$\begin{aligned}\Sigma_3(\sigma, l) &= \int_0^\infty \mathrm{d}z \left(\frac{\partial m_\pi}{\partial\sigma}\right)\left(\frac{\partial m_\pi}{\partial l}\right) \\ &= K(\kappa l - 1)\mathrm{e}^{-\kappa l}\left[\frac{m_\beta + 2(\sigma - m_\beta)\mathrm{e}^{-\kappa l} + m_\beta\mathrm{e}^{-2\kappa l}}{(1-\mathrm{e}^{-2\kappa l})^2}\right]\end{aligned} \quad (53)$$

and $W(\sigma, l)$ is given by the analogue of (5), yielding

$$W(\sigma,l) = \bar{h}l + \tfrac{1}{2}(K\kappa + c)(\sigma - [\tau + m_\beta])^2 + \frac{K\kappa}{2}\left[\frac{4m_\beta(\sigma - m_\beta)\mathrm{e}^{-\kappa l} + 2(m_\beta^2 + [\sigma - m_\beta]^2)\mathrm{e}^{-2\kappa l}}{1 - \mathrm{e}^{-2\kappa l}}\right] \tag{54}$$

where $\tau = (h_1 - cm_\beta)/(c + K\kappa)$ is a measure of the deviation from the MF critical wetting phase boundary. We note from (51) that in the double-parabola approximation the lower stiffness Σ_1 is independent of the field σ. We now write $\sigma(\boldsymbol{y}) = \sigma_0 + \delta\sigma(\boldsymbol{y})$ where $\sigma_0 = \tau + m_\beta$ is the equilibrium value of $\sigma(\boldsymbol{y})$, and can expand the above functions about $\sigma = \sigma_0$. We further define an effective single-field model $\mathcal{H}_{\mathrm{eff}}[l]$ via

$$\exp(-\beta\mathcal{H}_{\mathrm{eff}}[l]) = \int \mathcal{D}(\delta\sigma)\exp(-\beta\mathcal{H}^{(2)}[\sigma, l]) \tag{55}$$

and note that in the double-parabola approximation this trace can be performed exactly as only Gaussian terms are involved.

The resultant Hamiltonian at the square gradient level is identical in form to the FJ model (3) with $\mathcal{H}_{\mathrm{eff}}[l] = \int \mathrm{d}\boldsymbol{y}\,\{\frac{1}{2}\Sigma_{\mathrm{eff}}(l)(\nabla l)^2 + W_{\mathrm{eff}}(l)\}$. The effective binding potential is identical at all orders to that predicted by the FJ theory with

$$W_{\mathrm{eff}} = \bar{h}l + \frac{2K\kappa m_\beta\tau\mathrm{e}^{-\kappa l} + [K\kappa\tau^2 + K\kappa\mathcal{G}m_\beta^2]\mathrm{e}^{-2\kappa l}}{1 - \mathcal{G}\mathrm{e}^{-2\kappa l}} \tag{56}$$

where $\mathcal{G} = (c - K\kappa)/(c + K\kappa)$ and $0 < \mathcal{G} < 1$ [27]. The effective stiffness has the same form as the corresponding FJ parameter

$$\Sigma_{\mathrm{eff}} = \Sigma_{\alpha\beta} + 2K\kappa m_\beta\tau\mathrm{e}^{-\kappa l} + (s_{20} + s_{21}\kappa l)\mathrm{e}^{-2\kappa l} + \cdots \tag{57}$$

but in contrast with the binding potential, the coefficients s_{20}, s_{21} (and higher-order coefficients) are different from those found in the FJ theory with

$$\begin{aligned} s_{20} &= \tfrac{1}{2}K\kappa m_\beta^2(9 - 2\mathcal{G} - \mathcal{G}^2) + 2K\kappa\tau^2 \\ s_{21} &= K\kappa m_\beta^2(2\mathcal{G} - 4). \end{aligned} \tag{58}$$

The modifications to the leading-order term, s_{21}, can be directly attributed to the contribution from $\Sigma_3(\sigma, l)$—hence if Σ_3 in (53) is replaced by zero we precisely recover the FJ expression for s_{21}. Conversely the lower stiffness $\Sigma_1(l)$ only contributes to s_{20} and higher-order terms, in complete accord with our earlier observations based on the RG equations.

It is now straightforward to compare the predictions for the stiffness instability mechanism from the two-field theory with those from the original single-field theory. If the capillary parameter satisfies $\frac{1}{2} < \omega < 2$, which we believe to be the case near critical wetting, then FJ predict that the important quantity is [7, 8]

$$\mathcal{Q} \approx \frac{|s_{21}|}{w_{20} + s_{20}} \tag{59}$$

where w_{20} is the coefficient of the $\mathcal{O}(\mathrm{e}^{-2\kappa l})$-term in the binding potential. For sufficiently large $\mathcal{Q}$ the bare critical wetting transition is predicted to be driven fluctuation-induced first order, while for smaller $\mathcal{Q}$ the transition remains critical. Here we need not concern ourselves with determining the tricritical value separating these two regimes. Rather we simply compare the value of the parameter in our effective theory, $\mathcal{Q}_{\mathrm{eff}}$ say, with the corresponding FJ prediction, which we denote $\mathcal{Q}_{\mathrm{FJ}}$. Terms proportional to τ vanish on the approach to the transition so that $\mathcal{Q}$ is essentially just a function of the surface enhancement c. We find that for all c which are consistent with MF critical wetting $\mathcal{Q}_{\mathrm{eff}} > \mathcal{Q}_{\mathrm{FJ}}$. Hence we are more likely to be in the fluctuation-induced first-order regime and so the stiffness instability mechanism is

strengthened by the inclusion of a lower field in our interface model. The size of the increase is relatively small with $\mathcal{Q}_{\rm eff}$ typically 10–20% larger than the corresponding $\mathcal{Q}_{\rm FJ}$; however, recall a change of this magnitude in the other direction would have greatly reduced the applicability of the mechanism.

Hence we conclude that including a second field in the interface model tends to strengthen the instability mechanism predicted by FJ. We have further determined that the important changes are due to the cross-term stiffness Σ_3, with the lower field stiffness Σ_1 having little impact on the results.

5. Discussion and conclusions

In this paper we have studied the effect of combining several of the recent advances in effective interface models for wetting transitions, namely position-dependent stiffness coefficients and multi-field theories, to determine their impact on complete and critical wetting in three dimensions. Much of our analysis has been based on a nonlinear RG scheme which for the first time allows for both multiple fields and position-dependent stiffnesses. We have shown that the coupled flow equations arising from this RG scheme can be cast into a compact matrix form (35), (36).

We have used the RG to study the renormalization of the capillary parameter for complete wetting which has previously been predicted for simple two-field models. In particular we derived a new expression for the capillary parameter, which includes nonlinear terms which have not previously been accessible. We have further determined the transient form of the capillary parameter during the RG flow, which has not been observed before. However, the fixed-point value which is essential for determining critical behaviour is shown to be identical to that previously predicted. Thus our analysis shows that the capillary parameter renormalization is a robust mechanism.

Finally we have examined the effect of including extra fields on the Fisher–Jin prediction of a stiffness instability mechanism near critical wetting. Motivated by the RG equations we have used a simple double-parabola calculation to show that the additional field strengthens the instability mechanism. Hence the likelihood of finding fluctuation-induced first-order wetting transitions is increased. We have shown that the important parameter in this strengthening is the cross-term stiffness Σ_3, which also yields the dominant position-dependent contribution to the stiffness matrix.

Acknowledgments

The author would like to thank Dr A O Parry and Professor J O Indekeu for fruitful discussions over a number of years. This research has been supported in part by the Nuffield Foundation (NUF-NAL 99).

References

[1] Dietrich S 1988 *Phase Transitions and Critical Phenomena* vol 12, ed C Domb and J L Lebowitz (London: Academic)
[2] Parry A O 1996 *J. Phys.: Condens. Matter* **8** 10 761
[3] Parry A O and Swain P S 1998 *Physica* A **250** 167
[4] Lipowsky R, Kroll D M and Zia R K P 1983 *Phys. Rev.* B **27** 449
[5] Brézin E, Halperin B I and Leibler S 1983 *Phys. Rev. Lett.* **50** 1387
[6] Fisher D S and Huse D A 1985 *Phys. Rev.* B **32** 247
[7] Fisher M E and Jin A J 1992 *Phys. Rev. Lett.* **69** 792

[8] Jin A J and Fisher M E 1993 *Phys. Rev.* B **47** 7365
Jin A J and Fisher M E 1993 *Phys. Rev.* B **48** 2642
[9] Boulter C J 1997 *Phys. Rev. Lett.* **79** 1897
Boulter C J 1998 *Phys. Rev.* E **57** 2062
[10] Gompper G and Kroll D M 1988 *Europhys. Lett.* **5** 49
Gompper G and Kroll D M 1988 *Phys. Rev.* B **37** 3821
[11] Lipowsky R and Fisher M E 1986 *Phys. Rev. Lett.* **57** 2411
Lipowsky R and Fisher M E 1987 *Phys. Rev.* B **36** 2126
[12] Binder K, Landau D P and Kroll D M 1986 *Phys. Rev. Lett.* **56** 2272
Binder K and Landau D P 1988 *Phys. Rev.* B **37** 1745
Binder K, Landau D P and Wansleben S 1989 *Phys. Rev.* B **40** 6791
[13] Parry A O and Boulter C J 1996 *Phys. Rev.* E **53** 6577
[14] Parry A O and Boulter C J 1994 *J. Phys. A: Math. Gen.* **27** 1877
Parry A O and Boulter C J 1995 *Physica* A **218** 77
[15] Varea C and Robledo A 1999 *Physica* A **268** 391
[16] Parry A O 1993 *J. Phys. A: Math. Gen.* **26** L667
[17] Fisher M E and Wen H 1992 *Phys. Rev. Lett.* **68** 3654
[18] Boulter C J and Parry A O 1995 *Physica* A **218** 109
[19] Binder K, Landau D P and Ferrenberg A M 1995 *Phys. Rev. Lett.* **74** 298
Binder K, Landau D P and Ferrenberg A M 1995 *Phys. Rev.* E **51** 2823
[20] Boulter C J and Parry A O 1996 *J. Phys. A: Math. Gen.* **29** 1873
[21] Flesia S 1997 *Europhys. Lett.* **38** 113
[22] Parry A O, Boulter C J and Swain P S 1995 *Phys. Rev.* E **52** R5768
[23] Pandit R and Wortis M 1982 *Phys. Rev.* B **25** 3226
[24] Ma S-K 1976 *Modern Theory of Critical Phenomena* (Reading, MA: Benjamin)
[25] Lipowsky R 1988 *Europhys. Lett.* **7** 255
[26] Lipowsky R 1984 *Z. Phys.* B **55** 345
[27] Nakanishi H and Fisher M E 1982 *Phys. Rev. Lett.* **49** 1565